https://doi.org/10.17221/124/2017-VETMED

Computed tomographic features of tracheal shapes and dimensions in awake dogs

S. Lim[1], J. Jeong[1], H.G. Heng[2], S. Sung[1], Y. Choi[1], H. Oh[1], K. Kim[1], Y. Cho[3], Y. Jung[4], K. Lee[1]*

[1]Chonbuk National University of Veterinary Clinical Science, Iksan-si, Republic of Korea
[2]Purdue University College of Veterinary Medicine, West Lafayette, USA
[3]College of Health Sciences, Cheongju University, Cheongju, Republic of Korea
[4]Research Ethics Center, Office of Research Management, Korea University, Seoul, Republic of Korea

*Corresponding author: kclee@chonbuk.ac.kr

ABSTRACT: There are several reports in the veterinary literature on tracheal assessment; however, there is a lack of studies on the trachea in voluntarily breathing dogs. The aim of this study was to describe the natural shape of the trachea in awake dogs and to assess tracheal dimensions and the width-to-height ratio. Thoracic computed tomographic images of awake small breed dogs without any signs of respiratory malfunction (n = 19) were evaluated. Each trachea was categorised into one of four different shapes: circular, horseshoe, crescent or focal dorsal invagination. The circular shape was prominent, particularly in the thoracic inlet and intrathoracic area, while the horseshoe shape was also normally present. In this group of normal dogs, there were no crescent-shaped tracheas, but focally invaginated tracheas were observed. The mean tracheal heights at five locations, namely the caudal endplate of the fourth cervical vertebra, cranial endplate of the seventh cervical vertebra, mid-body of the first thoracic vertebra, mid-body of the third thoracic vertebra, and 1 cm cranial to the carina were 9.12, 8.96, 9.34, 9.88 and 10.16 mm, respectively. The widths at these same sites were 12.26, 10.42, 10.07, 9.82 and 10.23 mm, respectively. The width-to-height ratios of each tracheal location were 1.38, 1.20, 1.10, 1.01 and 1.03, the last two of which are consistent with the circular shape of the intrathoracic trachea. Multi-detector computed tomography under non-general anaesthesia is a non-invasive and unparalleled imaging tool for describing tracheal appearance in healthy awake dogs.

Keywords: anaesthesia-free procedure; trachea; shape; diameter; computed tomography

The trachea is the semi-rigid airway that runs from the cartilage of the larynx to the carina where it bifurcates into the principal bronchi. It consists of the dorsal trachealis muscles and incomplete C-shaped hyaline cartilaginous rings. Histologically, the tracheal wall consists of inner mucosa, submucosa, a fibrocartilaginous ring and outer adventitia or serosa (Sura and Durant 2012). The number of cartilaginous rings varies from 36 to 45 in mixed breed dogs (Dabanoglu et al. 2001).

Tracheal morphology has been classified as circular, horseshoe, elliptical, triangular, D- or U-shaped in previous human studies (Griscom 1983; Baer et al. 1987). Some human reports also described a frown-like shape instead of a crescent shape (Boiselle et al. 2009; Sverzellati et al. 2009). The posterior membrane, similar to the canine dorsal trachealis membrane, seems to be the major structure responsible for variation in tracheal shape, because the anterior and lateral portions of the trachea are strongly supported by the cartilaginous structure. The description of cross-sectional tracheal shapes in veterinary medicine does not correspond to the terminology used in humans.

Computed tomography (CT) has been introduced as the imaging modality of choice for stent selec-

https://doi.org/10.17221/124/2017-VETMED

tion, and is routinely performed before and after tracheal stent implantation in human medicine (Williams et al. 2016). CT provides cross-sectional imaging and three-dimensional information free of superimposition of the entire trachea. In animals, general anaesthesia is commonly required for CT studies in order to reduce motion artefacts. In these instances, respiratory rates and rhythms and tidal volume are controlled, but this is an unnatural condition. A previous CT study in non-anesthetised dogs with primary tracheal obstruction described tracheal abnormalities in cases of tracheal diseases (Stadler et al. 2011). The authors concluded that non-anaesthetic CT scans could be used to provide a definitive diagnosis of upper airway obstruction. To the best of our knowledge, there have not been any reports demonstrating normal tracheal morphology and dimensions in awake dogs breathing voluntarily using CT.

The purposes of this study were to describe the morphology (natural shapes) of the trachea in awake dogs and to evaluate tracheal dimensions. We hypothesised that a variety of tracheal shapes would be observed in normal awake small and medium dogs during voluntary respiration.

MATERIAL AND METHODS

Case selection and patient preparation. Thoracic CT images of awake dogs (n = 41) were chosen from the medical records of Chonbuk National University Animal Medical Centre from 2010 to 2011. Among them, 19 patients were selected for this study. Inclusion criteria for the patients were as follows: (1) CT scans without any anaesthesia or sedation, (2) no history of respiratory clinical signs and (3) no noted tracheal disease. All patients with poor quality CT images were excluded. Signalments such as age, sex, breed and body weight, the presenting history, clinical signs and haematology and serum chemistry profiles were available for evaluation.

Using a spiral scanner (Somatom Plus 4, Siemens, Munich, Germany; Light speed QX/i, GE Medical Systems, Milwaukee, USA) at 121–140 kVp and 110 mAs, thoracic CT images were obtained in lateral or sternal recumbency, in whichever position the patients felt most comfortable. Imaging parameters included 3-mm-slice thickness, a pitch of 1 : 1 and 0.7-mm-reconstruction intervals. No chemical anaesthetic or sedative procedures were performed. For immobilisation, safet, and security, patients were wrapped in a towel and taped, or just taped on the CT table depending on their level of cooperation (Figure 1). The towel method was based on a previous non-anaesthetic CT study of pelvic fracture in dogs (Lee et al. 2012). Once the animal was restrained with medical tape on the CT table, respiratory condition and comfort were monitored before and during the CT study. The patients were not tightly wrapped so that they could breathe naturally.

Evaluation of the CT images. CT images were uploaded to a picture-archiving and communication system (PACS). The trachea images were reviewed by a board-certified radiologist (HGH) and classified into four shapes (Figure 2): circular, horseshoe, crescent or focal dorsal invagina-

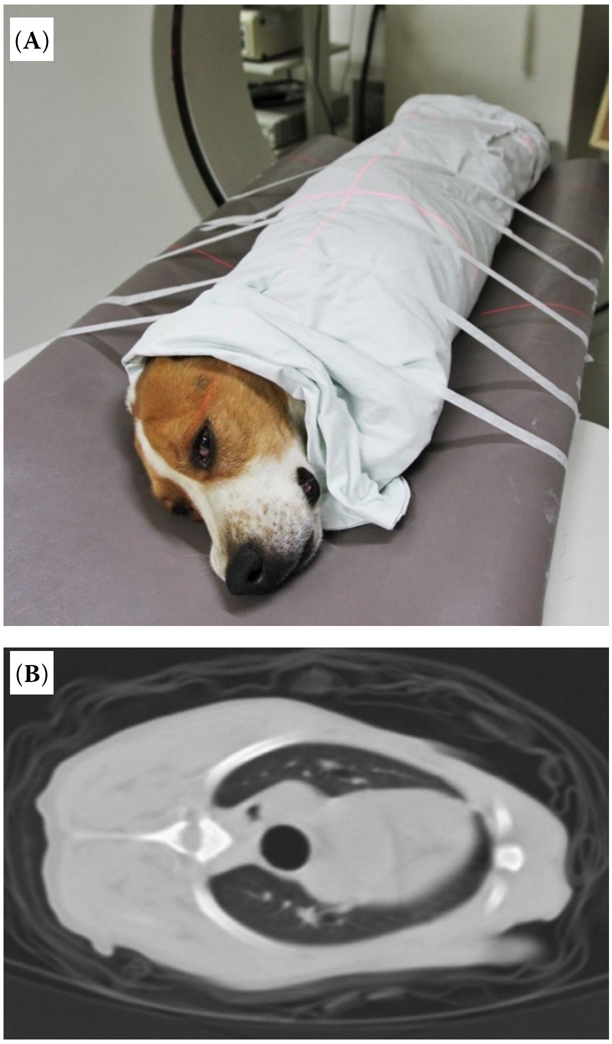

Figure 1. Physical restraint: The dog was wrapped in a towel and taped on the CT table (**A**). CT image of the dog wrapped and taped on the table (**B**)

https://doi.org/10.17221/124/2017-VETMED

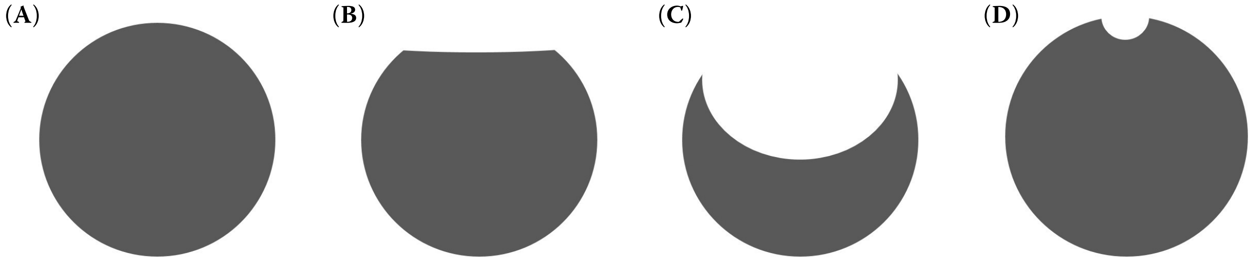

Figure 2. Four different trachea shapes: circular (**A**), horseshoe (**B**), crescent (**C**) and focal invaginated (**D**)

tion based on cross-sectional appearance (Boiselle et al. 2009). The tracheal height and width were measured at five locations: the caudal endplate of the fourth cervical vertebra (C4), cranial endplate of the seventh cervical vertebra (C7), mid-body of the first thoracic vertebra (T1), mid-body of the third thoracic vertebra (T3) and 1 cm cranial to the carina, which were similar to a recent publication reporting the use of CT and fluoroscopy to carry out tracheal diameter measurements (Williams et al. 2016). The trachea width-to-height (W/H) ratios were calculated. Descriptive statistics and *t*-tests were performed to summarise the mean tracheal height and width using SPSS software (IBM SPSS Statistics 20.0 for Windows; IBM Co., Somers, USA). *P*-values of less than 0.05 were considered to indicate statistical significance.

RESULTS

A total of 19 dogs met the inclusion criteria, six of which were male (three neutered males) and 13 of which were female (eight spayed females). The breeds included were Poodle (n = 4), Maltese (n = 3), Shih Tzu (n = 3), Schnauzer (n = 3), Yorkshire terrier (n = 3), Miniature pinscher (n = 1), Pointer (n = 1) and Pomeranian (n = 1). The mean age was 8.3 ± 3.0 years (range, two to 14 years) and the body weight was 5.1 ± 2.3 kg (range, 2 to 10 kg). No remarkable findings were found in the blood profiles of any of the selected patients, and no repeat CT scans were required for any patients. Three dogs were in sternal recumbency, seven were in right lateral recumbency and nine were in left lateral recumbency, wherever each patient was most comfortable. The shapes and sizes of the trachea in sternal recumbency did not have any distinct differences from tracheas in both right and left lateral recumbency. Each trachea was evaluated based on its cross-sectional morphology (Figure 3). Half of the tracheas were circular and the other half were horseshoe-shaped in the cervical region. The circular shape was dominant in the intrathoracic area with a percentage of 78.9% compared to 21.1% with a horseshoe shape. No crescent-shaped tracheas were found, and focal invagination was found in the cervical area with a frequency of 18.8% (Table 1).

There was a mild decrease in the average height at the thoracic inlet (T1), then a mild increase toward the caudal tracheal region (cranial to the carina). In contrast, the average width gradually decreased towards T3 and mildly increased towards the carina. These changes are consistent

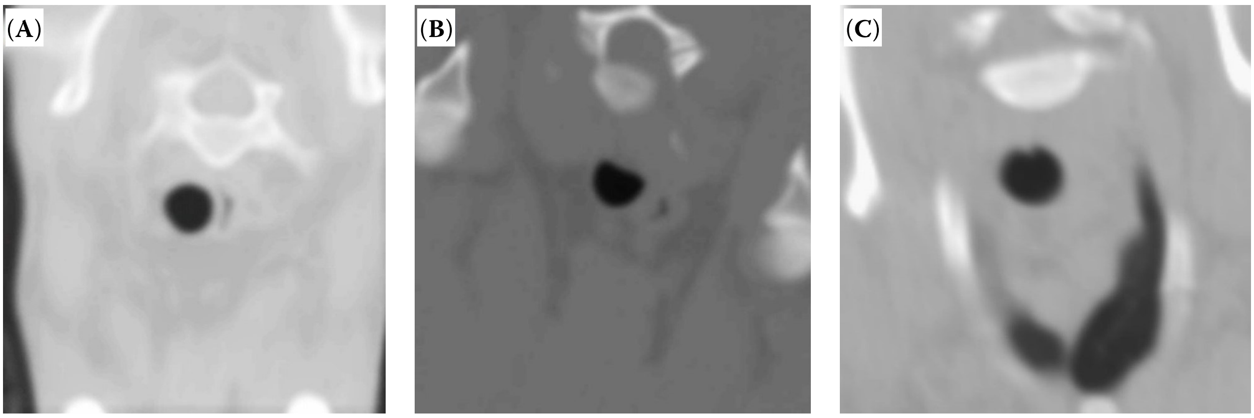

Figure 3. Tracheal cross-sectional appearances: circular (**A**), horseshoe (**B**) and focally invaginated shapes (**C**)

https://doi.org/10.17221/124/2017-VETMED

Table 1. Frequency of the tracheal shapes at five different locations. Values are presented as *n* (%)

Tracheal location	Tracheal shape				
	circular	horseshoe	crescent	focal dorsal invagination	total frequency
Caudal endplate of C4	3 (50.0%)	2 (33.3%)	0 (0.0%)	1 (16.7%)	6 (100.0%)
Cranial endplate of C7	6 (37.5%)	7 (43.7%)	0 (0.0%)	3 (18.8%)	16 (100.0%)
Mid-body of T1	12 (63.1%)	6 (31.6%)	0 (0.0%)	1 (5.3%)	19 (100.0%)
Mid-body of T3	15 (78.9%)	4 (21.1%)	0 (0.0%)	0 (0.0%)	19 (100.0%)
Cranial to carina	15 (78.9%)	4 (21.1%)	0 (0.0%)	0 (0.0%)	19 (100.0%)

with the width-to-height ratio becoming 1.01 at the T3, which directly reflects the high frequency of circular-shaped tracheas observed toward the intrathoracic region (Table 2). There were no statistical differences found in the tracheal shapes and sizes with respect to the body weight, gender, breed and age of the patients.

Subjectively we analyzed the axial rotation of the thoracic inlet and intrathoracic trachea, compared to the long axis of the spinous process, in different recumbency. The intrathoracic trachea and about half of the trachea at thoracic inlet have no axial rotation. In right lateral recumbency, two tracheas at thoracic inlet rotate anticlock-wise to the spinous process. In left lateral recumbency, five rotate clock-wise and one rotates anticlock-wise at thoracic inlet. In sternal recumbency, one trachea rotates clock-wisely at thoracic inlet. Among them, two clock-wise rotated tracheas in left recumbency and sternal recumbency moderately rotate over the angle of 30 degrees, and the other tracheas mildly rotate less than 30 degrees.

Table 2. The tracheal height, width and width-to-height ratio

Tracheal location	Tracheal shape		
	mean	SD	*P*-value
Height (mm)			
Caudal endplate of C4	9.12	2.48	0.00*
Cranial endplate of C7	8.96	2.38	0.00*
Mid-body of T1	9.34	2.30	0.00*
Mid-body of T3	9.88	2.41	0.00*
Cranial to carina	10.16	2.20	0.00*
Width (mm)			
Caudal endplate of C4	12.26	3.23	0.00*
Cranial endplate of C7	10.42	2.25	0.00*
Mid-body of T1	10.07	2.58	0.00*
Mid-body of T3	9.82	2.02	0.00*
Cranial to carina	10.23	2.03	0.00*
Width-to-height ratio			
Caudal endplate of C4	1.38	0.36	0.00*
Cranial endplate of C7	1.20	0.26	0.00*
Mid-body of T1	1.10	0.23	0.00*
Mid-body of T3	1.01	0.17	0.00*
Cranial to carina	1.03	0.22	0.00*

*Significance is set at $P < 0.05$

DISCUSSION

It is important to determine the morphological features and dimensions of the normal trachea in its natural state as this is the standard for diagnosing any tracheal abnormalities and for applying intubation, stenting, transplantation and endoscopic procedures. Although there have been several previous studies on tracheal appearance and diameter in normal dogs (Kara et al. 2004; Leonard et al. 2009; Kaye et al. 2015; Montgomery et al. 2015; Williams et al. 2016), its genuine shape in a natural state without any undesirable procedures such as general anaesthesia, sedation or excessive physical restraint is not known. The restraining method (wrapping and taping) was a simple and effective method to secure animals for non-general anaesthesia CT examination. Patients adapted quickly to the wrapping and taping method. Wrapping or taping method should be used cautiously as wrapping or taping too tight would be uncomfortable and could compromise respiration in sick animals.

The recumbence positions of the animals did not influence the morphology and size of the tracheas; thus, in the clinical setting for non-GA or sedated CT, this could be done in the position with which the animals were most comfortable. However, it is not clear if patients suffering from airway diseases would resemble normal dogs in this study; therefore, further studies evaluating recumbency effects on tracheal morphology and size in dogs with airway diseases are recommended.

https://doi.org/10.17221/124/2017-VETMED

In a subjective analysis on the axial rotation of the thoracic inlet and intrathoracic trachea in different recumbence positions, the direction of the tracheal axis was inconsistent between patients or between different recumbence positions, and the axial tracheal rotation seems to represent normal variation.

It is generally known that the lumen of the canine trachea is roughly circular, and the width-to-height ratio is approximately 1 : 1. However, dynamic variation in association with the respiratory cycle, and with pharyngeal, laryngeal and intrathoracic factors have also been described in the literature (Alexander 2008; Hayward et al. 2008). Anatomical differences and the degree of effort expended in inspiration and expiration were also identified as possible causes for tracheal shape variation in human medicine (Stern et al. 1993). In our study, the cranial portion of the trachea was generally either circular or horseshoe-shaped.

The tracheal shape in the thoracic inlet and intrathoracic region in dogs weighing less than 15 kg was more altered than that in the cervical region during expiration in a previous respiration study (Leonard et al. 2009). This is different from our observation where the shape of the caudal trachea appeared nearly circular, which we think is its normal shape. The major differences between the studies were the use of positive ventilation and CT imaging under general anaesthesia. Under general anaesthesia with positive pressure ventilation, the intrapleural pressure surrounding the trachea exceeds the intratracheal pressure during expiration so that the dimension of the intrathoracic trachea is reduced, which leads to invagination of the trachealis membrane. This could explain the difference in the tracheal shape found in the previous study compared to this study. In addition, the presence of an endotracheal tube makes it difficult to assess the genuine morphology and dimensions of the cervical trachea. Focal invagination in the cervical area in this study probably represents normal variation because none of the dogs had any underlying tracheal diseases.

Regarding the tracheal dimension, the degree of circularity directly corresponds to the W/H ratios of 1.01 and 1.03 at the mid-body of T3 and cranial to the carina, respectively. This W/H ratio was loosely analogous with previous values, which were approximately 1.14 in the intrathoracic trachea of a cadaver study (Dabanoglu et al. 2001) and 0.92 in a German shepherd study (Kara et al. 2004).

The height decreased near the thoracic inlet and slightly increased in a gradual manner caudally. The distance from the cranial to the carina is slightly greater than the most cranial aspect. However, the width decreased caudally and slightly increased cranial to the carina. This diameter, however, is still smaller than the most cranial aspect of the trachea measured. The changes of height and width resulted in a circular shape of the caudal trachea. The tendency for the dimensions to decrease near the thoracic inlet was well explained in a previous study. At the thoracic inlet level, the diameter and thickness of the tracheal rings are smallest as the trachea changes direction at the thoracic inlet. In addition, the trachea has the thinnest cartilage at this location so that it could readily collapse (Dabanoglu et al. 2001).

The adoption of a circular shape in the intrathoracic trachea mirrors the results of previous studies, but the increase in the height and width cranial to the carina was not observed in the previous large breed studies. This is probably because of the smaller tracheal dimensions of the small breed dogs in this study compared with that of the tracheal bifurcation.

It is important to understand the rough relationship between the tracheal dimension at each location and the animal size and breed. For instance, the thoracic inlet diameter was narrowest and the diameter grew with increasing distance from the thoracic inlet based on a study of the gross evaluation of 19 cadavers (Dabanoglu et al. 2001). The cadavers were from healthy adult mongrel dogs weighing about 16 kg with no history of airway disease. In a study on English bulldogs, the thoracic inlet was also found to have the narrowest diameter based on several different modalities including CT, radiography and endoscopy (Kaye et al. 2015); in contrast, the tracheal diameter continued to decrease toward the intrathoracic region in German shepherds (Kara et al. 2004).

This study has several limitations. First of all, only a small number of patients was analysed because it is difficult to collect thoracic CT data of normal dogs under non-general anaesthesia, especially when images of high quality without motion unsharpness are required. Another limitation of this study was that it was not known histologically if the horseshoe shape in the dogs was truly normal. The other limitation was that we were not able to precisely differentiate inspiratory or expiratory states during the acquisition of the CT study.

https://doi.org/10.17221/124/2017-VETMED

In conclusion, most of the cervical tracheas appeared circular or horseshoe-shaped as previously reported. However, the frequency of the circular shape was higher than that of the horseshoe shape in the thoracic inlet and intrathoracic area. Some dogs have a focal invagination of the dorsal tracheal membrane in the cervical region. None of the tracheas appeared crescent-shaped. CT imaging achieved under non-anaesthesia with minimal physical constraint is strongly recommended as the method of choice to visualise the authentic tracheal appearance of normal awake dogs without disturbing their natural state.

REFERENCES

Alexander K (2008): The pharynx, larynx, and trachea. In: Thrall DE (eds): Textbook of Veterinary Diagnostic Radiology. 6th edn. Elsevier Saunders, Missouri. 489–491.

Baer GA, Terho M, Tiensuu T (1987): Morphologic study of the adult trachea at the 7th and 12th ring. A study on specimens from 205 autopsies. Surgical and Radiologic Anatomy 9, 169–172.

Boiselle PM, O'Donnell CR, Bankier AA, Ernst A, Millet ME, Potemkin A, Loring SH (2009): Tracheal collapsibility in healthy volunteers during forced expiration: Assessment with multidetector CT. Radiology 252, 255–262.

Dabanoglu I, Ocal MK, Kara ME (2001): A Quantitative study on the trachea of the dog. Anatomia Histologia Embryologia 30, 57–59.

Griscom NT (1983): Cross-sectional shape of the child's trachea by computed tomography. American Journal of Roentgenology 140, 1103–1106.

Hayward N, Schwarz T, Weisse C (2008): The trachea. In: Schwarz T, Johnson V (eds): BSAVA manual of canine and feline imaging. BSAVA. 213–225.

Kara ME, Turan E, Dabanoglu I, Ocal MK (2004): Computed tomographic assessment of the trachea in the German shepherd dog. Annals of Anatomy 186, 317–321.

Kaye BM, Boroffka SAEB, Haagsman AN, Haar GT (2015): Computed tomographic, radiographic, and endoscopic tracheal dimensions in English Bulldogs with grade 1 clinical signs of brachycephalic airway syndrome. Veterinary Radiology and Ultrasound 56, 609–616.

Lee K, Heng HG, Jeong J, Naughton JF, Rohleder JJ (2012): Feasibility of computed tomography in awake dogs with traumatic pelvic fracture. Veterinary Radiology and Ultrasound 53, 412–416.

Leonard CD, Johnson LR, Bonadio CM, Pollard RE (2009): Changes in tracheal dimensions during inspiration and expiration in healthy dogs as detected via computed tomography. American Journal of Veterinary Research 70, 986–991.

Montgomery JE, Mathews KG, Marcellin-Little DJ, Hendrick S, Brown JC (2015): Comparison of radiography and computed tomography for determining tracheal diameter and length in dogs. Veterinary Surgery 44, 114–118.

Stadler K, Hartman S, Matheson J, O'Brien R (2011): Computed tomographic imaging of dogs with primary laryngeal or tracheal airway obstruction. Veterinary Radiology and Ultrasound 52, 377–384.

Stern EJ, Graham CM, Webb WR, Gamsu G (1993): Normal trachea during forced expiration: dynamic CT measurements. Radiology 187, 27–31.

Sura PA, Durant AM (2012): Trachea and bronchi. In: Tobias KM, Johnston SA (eds): Veterinary Surgery Small Animal. 2nd edn. Elsevier Saunders, Missouri. 1734–1751.

Sverzellati N, Rastelli A, Chetta A, Schembri V, Fasano L, Pacilli AM, Di Scioscio V, Bartalena T, De Filippo M, Zompatori M (2009): Airway malacia in chronic obstructive pulmonary disease: prevalence, morphology and relationship with emphysema, bronchiectasis and bronchial wall thickening. European Radiology 19, 1669–1678.

Williams JM, Krebs IA, Riedesel EA, Zhao Q (2016): Comparison of fluoroscopy and computed tomography for tracheal lumen diameter measurement and determination of intraluminal stent size in healthy dogs. Veterinary Radiology and Ultrasound 57, 269–275.

Received: September 20, 2017
Accepted after corrections: February 8, 2018